ISBN: 978-3-95450-132-8 doi:10.18429/JACoW-IPAC2014-TUPRI062

THE MODE MATCHING TECHNIQUE APPLIED TO THE TRANSVERSE BEAM COUPLING IMPEDANCE CALCULATION OF AZIMUTHALLY SYMMETRIC DEVICES OF FINITE LENGTH

N. Biancacci, E. Métral, B. Salvant, C. Zannini, CERN, Geneva, Switzerland
V. G. Vaccaro, University Federico II and INFN, Naples, Italy
M. Migliorati, L. Palumbo, University La Sapienza, Rome, Italy

Abstract

The infinite length approximation is often used to simplify the calculation of the beam coupling impedance of accelerator elements. This is expected to be a reasonable assumption for devices whose length is greater than the transverse dimension but may be a less accurate approximation for segmented devices. In this contribution we present the extension of the study of the beam coupling impedance of a finite length device to the transverse plane. In order to take into account the finite length, we decompose the fields in the cavity and in the beam pipe into a set of orthonormal modes and apply the Mode Matching Method to obtain the impedance. To validate our method, we will present comparisons between analytical formulas and 3D electromagnetic CST simulations.

INTRODUCTION

The impedance of finite length devices has been studied by other authors in the past mainly under the Leontovich or short inserts hypothesis [1–4]. The case under study is a cavity loaded with a toroidal insert of linear, stationary, homogeneous, isotropic and dispersive material as shown in Fig. 1. In the approach presented in this work we analyze the problem of determining the transverse dipolar impedance following the procedure as in [5, 6], i.e. applying the Mode Matching Method (MMM).

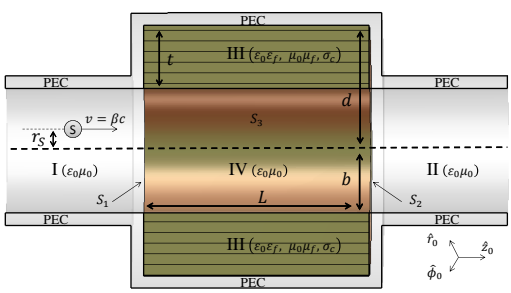

Figure 1: Structure under study: loaded cavity connected with two beam pipes.

MODE MATCHING METHOD

Given a volume enclosed in an ideal surface S the scattered electromagnetic fields $\overline{E}$ and $\overline{H}$ may be decomposed by means of the Helmholtz theorem in summation of irrotational and solenoidal modes which constitute a complete set of orthonormal functions [7].

Since the eigenvectors are determined by the geometry of the structure under study, the problem reduces into finding the unknown modal coefficients imposing the continuity of the EM field on the boundary surface S. The electromagnetic problem can be systematically solved recurring to the MMM as shown in detail in [5, 6].

With respect to the longitudinal impedance case, the transverse impedance calculation deserves more attention since the displaced source beam is coupled also to the TE modes in the cavity and the beam pipes.

BENCHMARKS

The MMM implementation has been extensively benchmarked in order to test the performance and reliability of the method itself. In the frame of these benchmarks, unless differently specified, we will consider the calculation of the transverse dipolar impedance in a cavity of pipe radius $b = 5$ cm and insert thickness $t = 25$ cm.

Basic tests have been done in order to ensure the method convergence as shown in Fig. 2 for a calculation of resistive wall impedance: increasing the number of longitudinal modes S and keeping constant the transverse modes P in the cavity, we can cover a wider frequency range and approach the expected resistive wall impedance curve. Similar considerations hold considering the convergence over the number of transverse modes P and fixed modes S.

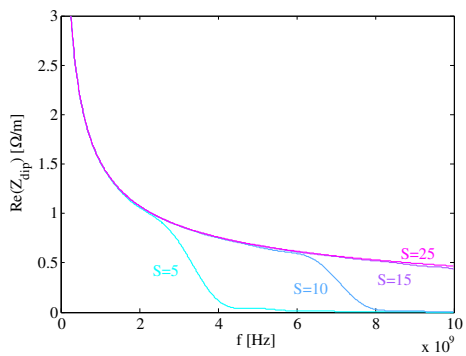

Figure 2: MMM convergence of the real part of the transverse impedance as a function of the longitudinal cavity modes S. MMM parameters: $L = 20$ cm, $\sigma_c = 10^6$ S/m, $\beta = 1$.

In the case of an empty cavity structure, we recover the modal distribution of a pillbox. Figure 3 shows the TM and TE modes excited in a cavity. As mentioned before, the transverse source current used to calculate the transverse dipolar

ISBN: 978-3-95450-132-8 doi:10.18429/JACoW-IPAC2014-TUPRI062

impedance couples both the TE and TM cavity modes. The insert has been taken with small but non-null conductivity in order to make the modes visible.

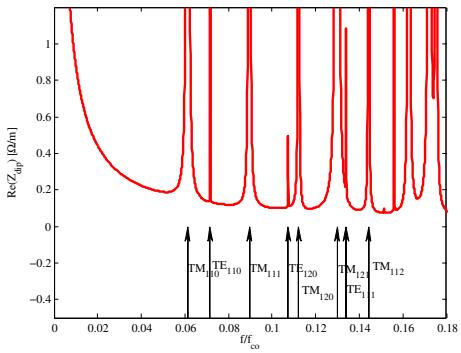

Figure 3: TM and TE modes excited in the dipolar impedance of an empty cavity. MMM parameters: $b = 1$ cm, $L = 20$ cm, $\sigma_c = 10^{-7}$ S/m, $\beta = 1$, $P = 10$, $S = 10$.

Varying the conductivity in the insert we benchmarked the MMM results with the classical resistive wall formulas for low frequency (LF) [8] and intermediate frequency range (IF) [9]. Figure 4 shows the comparison of the imaginary part of the dipolar impedance with the MMM calculation which is in good agreement. Analogous conclusions could be inferred also for the real part of the impedance.

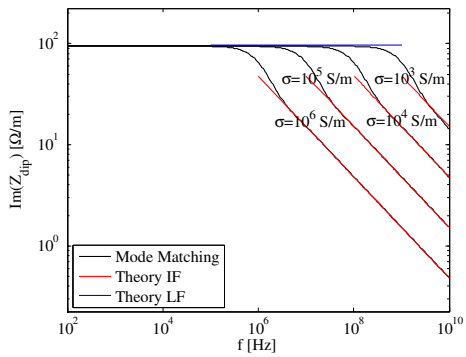

Figure 4: Comparison between MMM and classical theory of resistive wall impedance in the low (LF) and intermediate frequency range (IF). MMM parameters: $t = 500\,\mu$m, $L = 20$ cm, $\beta = 1$, $\sigma_c \in (10^3 - 10^6)$ S/m, $P = 10$, $S = 20$.

Decreasing the insert conductivity we can study the case of materials with small conductivity σ_c or equivalent conductivity $\sigma_{eq} = \omega\varepsilon_0\varepsilon_r \tan\delta$, where ε_r is the dielectric constant, ε_0 the vacuum permittivity, and $\tan\delta$ the loss tangent of the material. Figure 5 shows a comparison with CST Particle Studio 2013 [10] in case of a material with $\sigma_c = 10^{-2}$ S/m simulated with a bunch length of $\sigma_b = 3$ cm, wake length $L_{wake} = 20$ m using the *indirect testbeams* integration method. The agreement is very good.

The last benchmark but not least in importance has been done for the impedance dependence on beam velocity $v = \beta c$. This study is relevant for the correct modeling of the impedance in low energy machines like the CERN PSB and PS at the injection energy. Figure 6 shows the comparison

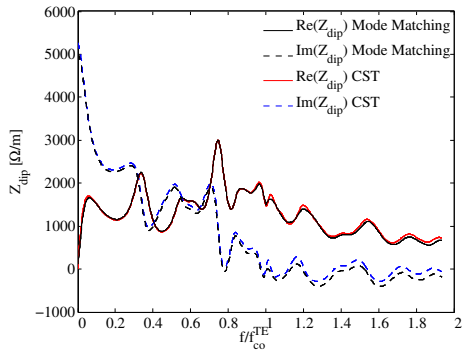

Figure 5: Comparison of MMM and CST for a poorly conducting insert. MMM parameters: $L = 20$ cm, $\sigma_c = 10^{-2}$ S/m, $\beta = 1$, $P = 15$, $S = 15$. CST parameters: $\sigma_b = 3$ cm, $L_{wake} = 20$ m, $N_{mesh} = 1.1 \cdot 10^6$ hexahedral.

of the MMM results as a function of the relativistic β with the available code "2D-Axi" for the study of a circular beam pipe geometry [11]. The discrepancy at low frequencies is due to the implementation of the PEC layer in 2D-Axi as a layer with high, but finite, conductivity. The overall agreement is otherwise satisfying.

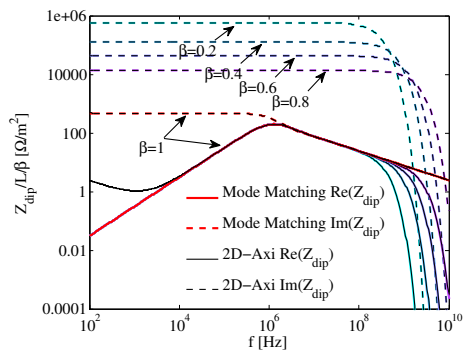

Figure 6: Comparison between MMM and the 2D-Axi code for different relativistic β. The transverse impedance is normalized over β. MMM parameters: $t = 0.5$ mm, $L = 20$ cm, $\sigma_c = 10^6$ S/m, $\beta = (0.2 - 1)$, $P = 25$, $S = 25$.

APPLICATIONS

The developed model allowed for the study of very thin inserts whose simulation is usually challenging in particle simulators like CST.

A resonant behavior was observed and studied for the longitudinal impedance in [5,6]. A similar one is present also in the transverse impedance as shown in Fig. 7 and it is due to the interplay of the insert impedance with the inductive load of the beam pipe below the TE_{11} cut-off frequency. The details of this effect are still under investigation.

Interesting is the length dependence of the broadband impedance at low frequency. Figure 8 shows the scaling of the transverse cavity impedance normalized to the length in case of a filling material with conductivity $\sigma_c = 10^6$ S/m. Well above the skin depth frequency (red line) the impedance calculated with a 2D code as 2D-Axi (blue curve) agrees

ISBN: 978-3-95450-132-8 doi:10.18429/JACoW-IPAC2014-TUPRI062

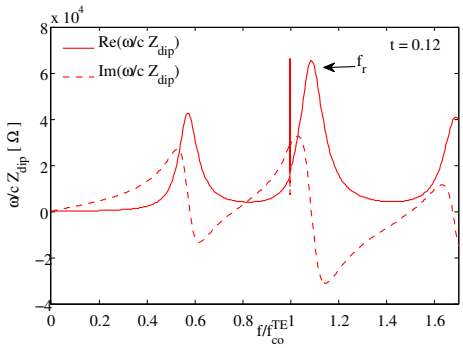

Figure 7: Kink in the dipolar impedance at the TE_{11} mode cut-off frequency. MMM parameters: $b = 5\,\text{cm}$, $t = 12\,\text{cm}$, $L = 1/8\,\lambda_{co}^{TE}$, $\sigma = 10^{-2}$ S/m, $\beta = 1$, P=5, S=25.

with the MMM ones (black curves). Close to the skin depth frequency, the insert impedance does not scale linearly and shows an increase for shorter cavity lengths.

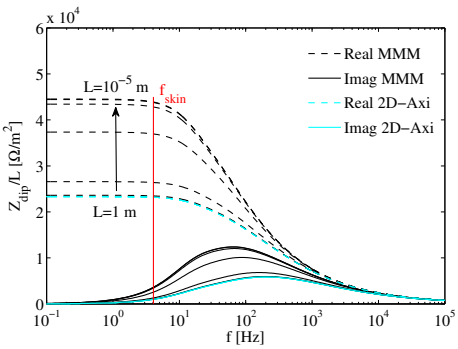

Figure 8: Impedance comparison between MMM (black curves) and the 2D-Axi model (blue curve) at low frequency. MMM parameters: $\sigma_c = 10^6$ S/m, $\beta = 1$, $P = 10$, $S = 10$.

This effect can be understood resorting to a simplified picture: above the skin depth limit, the current mainly flows on the device surface and the losses are increasing as the device length increases, i.e. linearly with the device length. On the other hand, the contribution of the capacitance between the two PEC edges that enclose the insert tends to increase for shorter lengths resulting in higher impedance per unit length.

Figure 9 shows a similar effect in the case of a ferrite TT2-111R as filling material. A comparison with CST is shown for a $\sigma_b = 4\,\text{cm}$, $L_{wake} = 3\,\text{m}$ and *direct* integration method. In this case, the inductance of the ferrite interacts with the capacitance of the two side plates. The capacitance increases for shorter lengths and the resonant frequency is therefore pushed downwards.

CONCLUSIONS

The Mode Matching Method has been successfully extended to the study of the transverse impedance of a cylindrical cavity loaded with a toroidal insert.

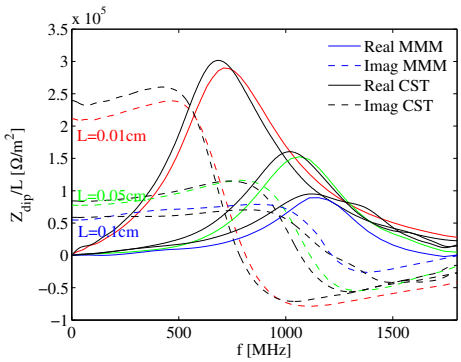

Figure 9: Comparison between MMM (blue, green and red lines) and CST (black lines) for a ferrite insert. MMM parameters: $\sigma_c = 10^6$ S/m, $\beta = 1$, $P = 30$, $S = 30$. CST parameters: $\sigma_b = 4\,\text{cm}$, $L_{wake} = 3\,\text{m}$, $N_{mesh} = 1 \cdot 10^6$ hexahedral.

An extensive set of benchmarks has been performed assessing the method reliability and good performance over a wide range of parameters.

A particular behavior has been observed at the cut-off frequency where the beam pipe load induces a resonant kink, and in the low frequency range for short inserts of lossy materials for which the usual linear scaling of the impedance with length is not valid due to the increase of the insert capacitance.

Further studies are ongoing for the method generalization to arbitrary geometries by means of general Eigenmode solvers.

ACKNOWLEDGEMENTS

The authors would like to acknowledge U. Niedermayer and O. Frasciello for the useful comments and suggestions.

REFERENCES

[1] B. Podobedov S. Krinsky and R. L. Gluckstern. Phys. Rev. ST-AB, 7:114401, Nov 2004.

[2] G. Stupakov. Phys. Rev. ST-AB, 8:044401, Apr 2005.

[3] R. L. Gluckstern and B. Zotter, CERN-AB-Note-2008-045, Geneva, Jul 2008.

[4] Y. H. Chin Y. Shobuda and K. Takata. Phys. Rev. ST-AB, 12:094401, Sep 2009.

[5] N. Biancacci, V. G. Vaccaro, E. Métral, B. Salvant, M. Migliorati, and L. Palumbo. Phys. Rev. ST Accel. Beams, 17:021001, Feb 2014.

[6] N. Biancacci, *Improved techniques of impedance calculation and localization in particle accelerators*, CERN-THESIS-2014-043, PhD Thesis, 2014.

[7] G. Franceschetti. *Campi elettromagnetici*. B. Boringhieri, 1983.

[8] K. Y. Ng. *Physics of Intensity Dependent Beam Instabilities*. World Scientific, New Jersey, NJ, USA, 2006.

[9] A. Chao. *Physics of Collective Beam Instabilities in High Energy Accelerators* Wiley, 1993.

ISBN: 978-3-95450-132-8 doi:10.18429/JACoW-IPAC2014-TUPRI062

[10] CST, Computer Simulation Technology, www.cst.com

[11] N. Mounet and E. Métral, CERN-BE-2009-039, CERN, Geneva, Switzerland, Nov 2009.